Int.J.Curr.Microbiol.App.Sci (2015) 4(11): 211-225

International Journal of Current Microbiology and Applied Sciences
ISSN: 2319-7706 **Volume 4 Number 11 (2015) pp. 211-225**
http://www.ijcmas.com

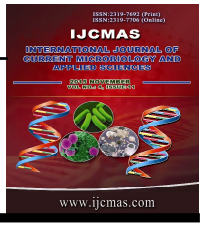

Original Research Article

Spectroscopic (FT-IR, FT-Raman & UV-Vis) and Density Functional Theory Studies of Cefadroxil

Kesavan Muthu[1]*, K. Gunasekaran[1], A.Kala[2], P. Govindasamy[3,6], P.Rajesh[4] and P.P. Moorthi[5]

[1]CAS in Crystallography and Biophysics, University of Madras (Guindy Campus), Chennai 600025, India
[2]Department of Physics, Govt Arts College for Men-Nandanam, Chennai 600035, India
[3]Department of Physics, Karpagam University, Eachanari, Coimbatore 641021
[4]Department of Physics, Meenakshi Academy of Higher Education, Research, Faculty of Humanities and Science, Meenakshi University, Chennai 600078, India
[5]PG and Research Department of Physics, Pachaiyappa's College, Chennai 600030, India
[6]Government Arts College –Dharmapuri636705, India
**Corresponding author*

Keywords

HOMO-LUMO, UV, DFT

A B S T R A C T

The Fourier transform infrared (FT-IR) and Fourier transform Raman (FT-Raman) spectra of the title molecule in solid phase were recorded in the region 4000–400 cm^{-1} and 4000–100 cm^{-1}respectively. The geometrical parameters and energies were investigated with the help of Density Functional Theory (DFT) employing B3LYP method and 6-311G(d, p) basis set. The analysis was supported by electrostatic potential maps and calculation of HOMO-LUMO, UV, FT-IR and FT-Raman spectra of cefadroxil were calculated and compared with experimental results. Thermodynamic properties like entropy, heat capacity, have been calculated for the molecule.

Introduction

Cefadroxil is a semi-synthetic p-lactam antibiotic from the group of Cephalosporin's antibiotic glass of drugs. Cefadroxil is chemically designated as (6R, 7R)-7-{[(2R)-2-amino-2-(4-hydroxyphenyl) acetyl] amino}-3-methyl-8-oxo-5-thia-1azabicyclo [4.2.0]oct-2-ene-2-carboxylic acid with molecular formula $C_{16}H_{17}N_3O_5S$. Cefadroxil is used to treat a variety of infections due to gram-positive and gram-negative bacteria (Zayed and Abdallah, 2004).

Cefadroxil is also useful for serious infections caused by susceptible strains of micro-organisms in lower respiratory infections, genitor-urinary infections, gynaecologic infections, skin infections and nervous system infections. This antibiotic works by inhibiting bacterial cell wall biosynthesis and are active against a wide range of both gram-positive and gram-negative bacteria. A positive feature of this drugs is that it display a resistance to

penicillinases and useful to treat infections that are resistant to penicillin derivatives.

Most of the antibiotics, including cefadroxil, and their decomposition products contain electron donor groups that can bind naturally-occurring metal ions in vivo. Metal ions form chelates with these antibiotics and reduce their intestinal absorption. It was reported that cefadroxil can form complexes with different metal ions (Zayed and Abdallah, 2004; Mrozek-Lyszczek, 2004). The interaction between cefadroxil and different metal ions was characterized by capillary electrophoresis (Auda *et al.,* 2009). Pharmacological studies in adults have demonstrated that cefadroxil is more slowly absorbed and has lower peak serum concentrations, longer serum half-life values, and slower urinary excretion than cephalexin when given in equivalent doses (Hartstein *et al.,* 1977; Pfeffer *et al.,* 1977). Substantial concentrations of cefadroxil are present in urine for at least 12 h after administration of a 500-mg dose.

Literature survey reveals that so far there is no complete experimental and theoretical study for the title compound cefadroxil. In this work, we mainly focus on the detailed spectral, vibrational assignments and thermodynamic properties based on the experimental Fourier transform infrared (FT-IR) and Fourier transform Raman (FT-Raman) spectra as well as DFT/B3LYP calculations for cefadroxil. Conformational analysis is the examination of the position of a molecule and the energy changes it HOMO and LUMO analysis has been used to elucidate the information regarding the charge transfer within the molecule. Finally, the UV-Vis spectra and the electronic absorption properties were explained and illustrated from the frontier molecular orbitals. Here, the calculated results have been reported in the text. The experimental and theoretical results supported each other and the calculations are valuable for providing insight into the vibrational spectra and molecular properties.

Experimental details

The compound cefadroxil under investigation was obtained from the Lancaster Chemical Company of UK with purity of 99% and it was subjected for the various spectral measurements. In room temperature the Fourier transform infrared spectra of cefadroxil was recorded in the region 4000–400 cm^{-1} at a resolution of ±1 cm^{-1} using BRUKER IFS-66V Fourier transform spectrometer equipped with a MCT detector, a KBr beam splitter and global source. The FT-Raman spectrum was recorded withFRA-106 Raman accessories in the region 4000-100 cm^{-1}Nd: YAG laser operating at 200mWpowers with 1064 nm excitation was used as a source. The UV–Visible absorption spectrum of the sample was recorded using a Shimadzu UV-1800 PC, UV-Vis spectrophotometer in the range 200–400 nm using water as solvent.

Methods of analysis

The molecular geometry optimization and vibrational frequency calculations were carried out for cefadroxil, using GAUSSIAN 03W software package (Frisch *et al.,* 2004), Becke's three parameter exchange functional (B3) (Becke, 1992, 1993) and combination with the correlation functional of Lee, Yang and Parr (LYP) (Lee *et al.,* 1988) with standard 6-311G(d,p) basis set. The potential energy distribution (PED) was calculated to each corresponding observed frequency using VEDA 4 program (Jamroz, 2004) and it shows the reliability and accuracy of the spectral analysis. The atomic charge, electric dipole moment, HOMO, LUMO and other thermodynamic

parameters were also calculated theoretically. Finally, the calculated normal mode of vibrational frequencies will provide the thermodynamic properties through the principle of statistical mechanics.

Geometrical parameters

In order to find the most optimized geometry, the energies were carried out for cefadroxil using B3LYP/6-311G (d,p) method. The optimized molecular structure of cefadroxil calculated by DFT-B3LYP level with the 6-311G(d,p) basis set are listed in the table 1 in accordance with the atom numbering scheme given in figure 1. The calculated bond lengths and bond angles of cefadroxil as shown in table 1. It is seen that B3LYP level with 6-311G(d,p) basis set in general estimate same value of some bond angle, bond length and dihedral angles. The optimized calculated bond lengthsC_4-S_5, S_5-C_6 are larger and O_{24}-H_{40} are shorter. Further the result of our calculations very high bond length strong bond which is found to be C_4-S_5 (1.8528A°) and smaller value of bond length weak bond O_{24}-H_{40} (0.9628A°). In cefadroxil, the bond length of C_4-S_5 is 1.8528Å due to the presence of electron donating nature of methyl group. The bond angle C_7-C_8-O_{12} (136.73Å) of cefadroxil because of electron donating nature of methyl group. The magnitudes of the C–C bond lengths on benzene ring are ranged from 1.3892° to 1.3984A at B3LYP level, which is longer than double bond length of (C=C) but shorter than that of the single C–C bond length (1.5666A˚). While the introduction of the substituent groups (hydroxyl and tertiary methyl group) causes slight difference between them, it may be due to the satiric repulsion between hydroxyl and methyl group. The CCC bond angles in the benzene ring slightly distorted from the hexagonal geometry was revealed by the bond angle C_{18}-C_{19}-C_{20} (121.59°). As the crystal structure of the exact title compound is not available as yet, the optimized structure can only be compared with other similar systems.

Molecular electrostatic potential

Molecular electrostatic potential (MEP) is very useful in research of molecular structure with its physicochemical property relationship.MEP is very useful in studying the relation between the structure and activity (Monasterios *et al.,* 2006)**.**To predict reactive sites for electrophilic and nucleophile attack for the investigated compound, molecular electrostatic potential (MEP) was calculated at B3LYP/6-311G (d,p) optimized geometries. Red and blue areas in the MEP map refer to the electron-rich and electron-poor regions, respectively, whereas the green colour signifies the neutral electrostatic potential. The MEP surface provides necessary information about the reactive sites. Potential increases in the orderred < orange <yellow< green < blue. The colour code of these maps is in the range between -0.058a.u. (deepest red) to0.046a.u. (deepest blue) in compound, where blue indicates the strongest attraction and red indicates the strongest repulsion. The MEP diagram of cefadroxilis is shown in figure 2.

UV-visible spectral analysis

To understand the electronic transitions inCefadroxil molecule,TD–DFT/B3LYP/6–311G (d,p) level of theory has been used based on optimised geometry and only the molecule with singlet–singlet strong oscillators is reported. The experimental λ_{max} values are obtained from the UV–Vis spectrum recorded in methanol solvent is shown in figure 3 depicts the observed UV–Vis spectrum of cefadroxil molecule. The calculations were also carried out with

methanol solvent effect. The calculated absorption wavelengths (λ_{max}), experimental wavelengths,electron transition energies in the isolated gas phase and in methanol solvent are listed in table 2. Strong absorption peak observed at 273.22(in gas phase) nm and the experimental wavelength at 277nm and at 260.26nm (in methanol) is caused by $\pi \rightarrow \pi^*$ transitions and a weak band is observed at 235.18nm due to $\pi \rightarrow \pi^*$ transition respectively (Rajesh *et al.*, 2014). As concluded from the UV-Vis table 2, the maximum absorption wavelength corresponding to the electronic transition from HOMO–>LUMO (69%) and H–1–>LUMO (63%), H-1->L+1 (-20%), H->L (22%)with contribution. The observed transition from HOMO→LUMO is n →π*

Mulliken atomic charges

The Mulliken atomic charges were calculated by determining the electron population of each atom as defined by the basis function [Fliszar *et al.*, 1983; Jug *et al.*, 1991]. The Mulliken atomic charges of Cefadroxil molecule calculated by B3LYP/6-311G (d,p) basis set. Calculation of effective atomic charges plays an important role in the application of quantum chemical calculations to molecular systemswas shown in figure 4. The results of the calculated charges atB3LYP/6-311G (d,p) is listed in table 3. The charges depending on basis set are changed due to polarizability. The H_{26} and H_{42} atoms have more positive charges than any other atoms. This is due to the presence of electro negativity of oxygen atoms and nitrogen atoms the attracts of positive charge of hydrogen atoms from the oxygen and nitrogen atoms. The carbon and oxygen atoms are more negative charges than the other atoms due to electron accepting substitutions at that position in Cefadroxil. The result suggests that the atoms O, N and H atoms are electron acceptor and charge transfer takes place from O and N to H in Cefadroxil respectively.

Thermodynamic properties

The values of thermodynamic parameters such as zero-point vibration energy, thermal energy, specific heat capacity, rotational constants, entropy, and dipole moment of Cefadroxil by B3LYP/6-311G(d.p) and basis set are calculated and listed in table 4. The standard thermodynamic functions such as heat capacity, entropy and enthalpy are calculated using perl script THERMO.PL (Irikura K K *et al.*, 2002) and are listed in table 4. As observed from the table 4, the values of C_P, H and S increase with the increase of temperature from 100 to 1000 K, which is attributed to the enhancement of the molecular vibration as the temperature increases. The correlation equations between heat capacity, entropy, enthalpy changes and temperatures are being fitted by quadratic formulas and the corresponding fitting factors (R^2) for these thermodynamic properties are 0.9996, 0.9994 and 0.9995, respectively. The corresponding fitting equations are as follows and the correlation graphs of those are shown in figure 5.

$C_{p,m}^{o} = -7.307 + 0.10214\,T + 1.9217 \times 10^{-4}\,T^2$ ($R^2 = 0.9996$)

$S_m^{o} = 39.2300 + 0.6579\,T - 2.5157 \times 10^{-4}\,T^2$ ($R^2 = 0.9994$)

$H_m^{o} = 271.028 + 0.8633\,T - 2.3118 \times 10^{-4}\,T^2$ ($R^2 = 0.9995$)

All the thermodynamic data provide useful information to study the title compound. They compute the other thermodynamic energies according to the relationships of thermodynamic functions and estimate the directions of chemical reactions according to the second law of thermodynamics in thermo chemical field.Notice: all

thermodynamic calculations are done in gas phase and they could not be used in solution.

HOMO and LUMO analysis

Numerous organic molecules that containing conjugated π electrons are characterized and analyzed by means of vibrational spectroscopy(Ataly 2008; Vijayakumar 2008). In most cases, even in the absence of inversion symmetry, the strongest bands in the Raman spectrum are weak in the IR spectrum and vice versa. But the intermolecular charge transfer from the donor to accepter group thorough a single-double bond conjugated path can induce large variations of both the molecular dipole moment and the molecular polarizability, making IR and Raman activity strong at the same time.The experimental spectroscopic actions described above is very well accounted by *B3LYP/6-311G (d,p)* calculations in π conjugated systems that predict remarkably large Raman and infrared intensities for the same normal modes (Pihlaja *et al.,* 1994). It is also observed in title of molecule the bands in FT-IR spectrum have their counterparts in Raman shows that the relative intensities in IR and Raman spectra are comparable resulting from the electron cloud movement through π conjugated frame work from electron donor to electron acceptor groups. Highest occupied molecular orbital (HOMO) and lowest unoccupiedmolecular orbital (LUMO) are very significant parameters for quantum chemistry. Using these parameters we can determine the way, in which molecule interacts with other species hence, they are called the frontiers orbital. HOMO can be thought the outermost orbital containing donor electrons and energy of the HOMO is directly related to the ionization potential. On the other hand LUMO can be thought the innermost orbital containing free places to accept electrons and their energy is directly related to the electron affinity (Gece 2008).Energy gap between HOMO and LUMO orbital describe the chemical reactivity and kinetic stability of molecule (Lewis *et al.,* 1994; Uesugi *et al.,* 1997). Recently, the energy gap between HOMO and LUMO has been used to prove the bioactivity from intermolecular charge transfer (ICT) (Padmaja *et al.,* 2009; Sagdinc *et al.,* 2009). The graphical structures of interaction between HOMO and LUMO in Cefadroxil, with its energy by B3LYP/ 6-311 G(d,p)method are shown in figure 6. The HOMO and LUMO energy gap of Cefadroxil calculated by B3LYP/6-311 G(d,p) methods**.** According to B3LYP/6-311 G (d,p) calculation, the energy band gap (ΔE) of the molecule is about 4.4719 eV. Energy gap= 4.4719 eV, HOMO = 6.324 eV, LUMO = 1.852 eV.

Vibrational assignments

The title molecule consists of 42 atoms, hence undergoes 120 normal modes of vibrations, all are active in infrared and Raman spectra. The molecule under investigation possesses C_1 point group symmetry.

The experimental IR and Raman spectra are shown in figures.7 and 8, respectively. The calculated vibrational frequencies, potential energy distribution (PED) and approximate descriptions of normal modes are listed in table 5. Usually, scaling factors are introduced to modify the calculated frequency values.

O-H Vibration

The O-H group stretching vibrations which are appeared about 3400–3600 cm^{-1}[Silverstein *et al.,* 2005]. The O-H group vibrations, especially stretching and out-of plane deformation are likely to be the

most sensitive to the environment, so they show pronounced shifts in the spectra of the hydrogen-bonded species. In the IR spectra of the compound, the peak at 3507cm^{-1} was assigned to O-H stretching vibration that has been calculated at 3497cm^{-1}.

C-H Vibration

The hydrogen atoms left around the ring in Cefadroxil give rise to C-H stretching, C-H in-plane bending and C-H out- of-plane bending vibrations. The hetroatomic structure shows the presence of C-H stretching vibrations in the region 3100-3000cm^{-1}, which is the characteristic region for ready identification of C-H stretching vibrations [Sundaragaresan*et al.,* 2004], in this region, the bands are not affected appreciably by the nature of substitutions. Hence, the band at 3010 cm^{-1} in IR and3070cm^{-1} in Raman spectrum are assigned to C-H stretching vibrations in the title compound. The C-H in-plane and out-of-plane bending vibrations of the title compound have also been identified and listen in table 5.

C-C Vibrations

There are very wide fluctuations in intensity [Krishnakumar *et al.,* 1994] in the absorption bands due to aromatic structures in the1600 cm^{-1}-1430cm^{-1} region. In this study the bands between 1565 cm^{-1}, 1517 cm^{-1} and 1456cm^{-1}in FT-IR spectrum of Cefadroxil respectively. The higher percentage of potential energy distribution (PED) obtained for this group encouraging and confirms the assignments proposed in this study for C-C stretching vibrations of Cefadroxil. The calculated values at 1550 cm^{-1}, 1529cm^{-1} and 1452 cm^{-1} are in excellent agreement with the experimental value for the corresponding mode of vibrations

N-H Vibrations

The vibration for N-H stretching always occurs in the region 3450 cm^{-1} to 3250 cm^{-1}[Gunasekaran*et al.,* 2005]. In thepresent study the FT-IR band observed at 1415cm^{-1}are assigned to N-H asymmetricand symmetric stretching vibrations respectively. The theoretically assigned N-H vibrations areat 1419 cm^{-1} respectively.

C–O Vibration

Generally the C–O occurs in the region 1260 cm^{-1} to 1000 cm^{-1}[Erdogdu *et al.,* 2010 and Varsanyi, 1974]. In the present study, the bands observed at 1269 cm^{-1}and 1233 cm^{-1} in FT-IR spectra and a weak band obtained at 1272 cm^{-1} in FT-Raman spectrum is assigned as C–O stretching vibration. These vibrational assignments are in line with the B3LYP method. According to the literature, the C–O vibration is pushed to the lower region by the influence of other vibrations.In Cefadroxil C–O in plane bending vibration is found at 827 cm^{-1}and 766 cm^{-1} at B3LYP/6-31G(d, p) level, which is found mixed with the O–H deformation mode. These assignments are in good agreement with the literature value (Snehalatha *et al.,* 2009a,b).

C–N Vibration

Rajesh.P *et al.,* 2014.have observed the C–N stretching band at 1305 cm^{-1} in FTIR and 1307 cm^{-1} in FT-Raman spectra of Cefadroxil. Hence in the present investigation, FT-IR band observed at 1354 cm^{-1} and band at 1356 cm^{-1} in the FT-Raman spectrum of Cefadroxil are assigned to the C–N stretching mode of vibrations. The calculated values at 1357 cm^{-1}and 1300 cm^{-1} are in excellent agreement with the experimental value for the corresponding mode of vibrations.

Table.1 Optimized geometrical parameters of like bond length and bond angles of cefadroxil

Bond Length(Å)	B3LYP	Bond Angle (°)	B3LYP
N_1-C_2	1.4274	S_5-C_4-H_{27}	105.20
N_1-C_6	1.4872	N_1-C_6-S_5	112.79
N_1-C_8	1.4108	H_{26}-C_4-H_{27}	107.89
C_2-C_3	1.3506	C_4-S_5-C_6	96.360
C_2-C_9	1.5011	N_1-C_6-C_7	88.130
C_3-C_4	1.5088	N_1-C_6-H_{28}	113.38
C_3-C_{13}	1.4983	S_5-C_6-C_7	120.06
C_4-S_5	1.8528	S_5-C_6-H_{28}	107.48
C_4-H_{26}	1.0928	C_7-C_6-H_{28}	114.10
C_4-H_{27}	1.0894	C_6-C_7-C_8	85.980
S_5-C_6	1.8290	C_6-C_7-N_{17}	119.95
C_6-C_7	1.5666	C_6-C_7-H_{29}	112.01
C_6-H_{28}	1.0911	C_8-C_7-N_{17}	118.14
C_7-C_8	1.5482	C_8-C_7-H_{29}	111.71
C_7-H_{17}	1.4257	N_{17}-C_7-H_{29}	107.79
C_7-H_{29}	1.0921	N_1-C_8-C_7	91.661
C_8-O_{12}	1.1953	N_1-C_8-O_{12}	131.59
C_9-O_{10}	1.2033	C_7-C_8-O_{12}	136.73
C_9-O_{11}	1.3503	C_2-C_9-O_{10}	124.81
O_{11}-H_{30}	0.9678	C_2-C_9-O_{11}	114.57
C_{13}-H_{31}	1.0962	O_{10}-C_9-O_{11}	120.61
C_{13}-H_{32}	1.0961	C_9-O_{11}-H_{30}	108.76
C_{13}-H_{33}	1.0848	C_3-C_{13}-H_{31}	109.39
C_{14}-C_{15}	1.5469	C_3-C_{13}-H_{32}	109.33
C_{14}-O_{16}	1.2151	C_3-C_{13}-H_{33}	112.42
C_{14}-N_{17}	1.3695	H_{31}-C_{13}-H_{32}	106.69
C_{15}-C_{18}	1.5176	H_{31}-C_{13}-H_{33}	108.80
C_{15}-N_{25}	1.4813	H_{32}-C_{13}-H_{33}	110.02
C_{15}-H_{34}	1.0955	C_{15}-C_{14}-O_{16}	122.65
N_{17}-H_{35}	1.0148	C_{15}-C_{14}-N_{17}	113.43
C_{18}-C_{19}	1.3984	O_{16}-C_{14}-N_{17}	123.85
C_{18}-C_{23}	1.3977	C_{14}-C_{15}-C_{18}	112.81
C_{19}-C_{20}	1.3892	C_{14}-C_{15}-N_{25}	110.45
C_{19}-H_{36}	1.0858	C_{14}-C_{15}-H_{34}	103.95
C_{20}-C_{21}	1.3954	C_{18}-C_{15}-N_{25}	114.35
C_{20}-H_{37}	1.0831	C_{18}-C_{15}-H_{34}	107.99
C_{21}-C_{22}	1.3968	N_{25}-C_{15}-H_{34}	106.50
C_{21}-O_{24}	1.3647	C_7-N_{17}-C_{14}	122.08
C_{22}-C_{23}	1.3906	C_7-N_{17}-H_{35}	122.50
C_{22}-H_{38}	1.0862	C_{14}-N_{17}-H_{35}	114.96
C_{23}-H_{39}	1.0843	C_{15}-C_{18}-C_{19}	120.13
O_{24}-H_{40}	0.9628	C_{15}-C_{18}-C_{23}	121.72
N_{25}-H_{41}	1.0144	C_{19}-C_{18}-C_{23}	118.02
N_{25}-H_{42}	1.0167	C_{18}-C_{19}-C_{20}	121.59
C_2-N_1-C_6	126.54	C_{18}-C_{19}-H_{36}	119.52
C_2-N_1-C_8	130.93	C_{20}-C_{19}-H_{36}	118.88
C_6-N_1-C_8	94.271	C_9-C_{20}-C_{21}	119.63
N_1-C_2-C_3	117.16	C_{19}-C_{20}-H_{37}	121.41
N_1-C_2-C_9	116.69	C_{21}-C_{20}-H_{37}	118.95
C_3-C_2-C_9	126.00	C_{20}-C_{21}-C_{22}	119.60
C_2-C_3-C_4	117.44	C_{20}-C_{21}-O_{24}	117.57
C_2-C_3-C_{13}	126.17	C_{22}-C_{21}-O_{24}	122.81
C_4-C_3-C_{13}	116.36	C_{21}-C_{22}-C_{23}	120.08
C_3-C_4-S_5	112.08	C_{21}-C_{22}-H_{38}	119.98
C_3-C_4-H_{26}	111.27	C_{23}-C_{22}-H_{38}	119.92
C_3-C_4-H_{27}	111.30	C_{18}-C_{23}-C_{22}	121.05
S_5-C_4-H_{26}	108.80	C_{18}-C_{23}-H_{39}	120.12

Table.2 The UV-Vis Excitation Energy of Cefadroxil

TD-B3LYP/6-311G(d,p) Gas Phase		Expt. λ_{obs}	Major Contributions
λcal	E(eV)		
273.22	3.8908	277	HOMO->LUMO (69%)
260.26	4.0841	-	H-1->LUMO (63%)
235.18	4.3148	230	H-1->L+1 (-20%), H->L (22%)

Table.3 Natural bond analysis of cefadroxil

Atoms	Charge (eV)	Atoms	Charge (eV)	Atoms	Charge (eV)
N_1	0.490	C_{15}	-0.129	H_{29}	0.181
C_2	0.082	O_{16}	-0.357	H_{30}	0.245
C_3	-0.042	N_{17}	-0.394	H_{31}	0.128
C_4	-0.381	C_{18}	-0.055	H_{32}	0.126
S_5	0.143	C_{19}	-0.075	H_{33}	0.159
C_6	-0.130	C_{20}	-0.085	H_{34}	0.162
C_7	-0.073	C_{21}	0.157	H_{35}	0.234
C_8	0.358	C_{22}	-0.129	H_{36}	0.081
C_9	0.432	C_{23}	-0.033	H_{37}	0.105
O_{10}	-0.324	O_{24}	-0.359	H_{38}	0.092
O_{11}	-0.291	N_{25}	-0.464	H_{39}	0.096
O_{12}	-0.287	H_{26}	0.187	H_{40}	0.248
C_{13}	-0.267	H_{27}	0.168	H_{41}	0.209
C_{14}	0.387	H_{28}	0.169	H_{42}	0.210

Table.4 Thermodynamic properties of cefadroxil

Temperature	Entropy	Enthalpy	Heat Capacity
100	348.23	106.87	7.2700
200	438.63	158.87	20.610
298	511.43	209.55	38.670
300	512.73	210.52	39.060
400	580.41	261.92	62.710
500	643.91	307.69	91.250
600	703.51	346.12	124.00
700	759.33	377.91	160.25
800	811.57	404.32	199.41
900	860.51	426.42	240.97
1000	906.43	445.05	284.57

Table.5 Vibrational assignments of cefadroxil

B3LYP/ 6-311G(d,p)	Experimental		Vibrational Assignments+PED(%)
	FT-IR(cm^{-1})	FT-R(cm^{-1})	
3497	3507	-	υOH (100)
3465	-	-	υOH (100)
3458	-	-	υNH_2(100)
3450		-	υNH_2(99)
3419	3415	-	υNH_2 (99)
3199	3199	-	υCH (96)
3195	-	-	υCH (93)
3178		-	υCH (91)
3175	-	-	υCH (93)
3141	-	-	υCH (88)
3085	-	3070	υCH_2 (100)
3041	-	-	υCH (96)
3039	-	-	υCH_2 (99)
3013	3010	-	υCH_2 (100)
2961	-	-	υCH_2 (93)
2132	-	-	υOC (88)
2066	-	-	υOC (84)
2002	-	-	υOC (85)
1888	1898	-	υCC(69)
1785	-	-	υCC(60)
1781	-	-	υHNH (73)+ τHNCC(25)
1734	1736		υCC(42)
1683	1685	-	δHCC(44)
1642	-	1650	δNC (22)+ δHNC(53)
1606	-	-	δHCH(76) + τHCCC(16)
1550	1565	-	υCC(25) +δHCH(51) +δHCC(13)
1529	1517	-	δHCH(29)+ τHCCC(10)
1472	-	-	δHCH(64)
1468	-	-	τHCCC(47)+ δHNC(27)
1452	1456		υCC(43)+ δHOC(19)
1446	-	-	υOC (11)+ υNC(21)+ δHOC(27)
1441	-	-	δHCN(16)+ δHCC(16)
1435	-	-	δHCN (22)
1419	1415	-	υNC (18)+δHCN (22)+ δHCS(37)
1376	-	1393	υOC (47)+ δHCS(12)
1374	-	-	υCC(12)+ δHOC(14)+τHCSC(14)
1365			τHCSC(16)+υNC(16)
1357	1354	1356	υNC (23)+δHNC(13)
1336	-	-	υCC (10)+δHCS(13)+τHCSC(19)
1300	1309	-	δHNC(14)+ τHCCN(19)
1299	1284	-	υCC (70)+ τHCCN(27)

1252	1269	1272	δOC(13)+δHOC(21)
1251	1233	-	δHOC(36)+ δHCC(12)
1176	1198	1184	υNC (11)+ υOC(14)
1099	1094	-	υNC(12)
1077	1070	-	δCCC(45)
1068	1044	-	δCNC(10)
1010	1024	-	τHCCC(85)
985	984	-	τHCCC(76)+ τCCCC(11)
973	954	-	υCC(27)
878	-		γ OCCC(13)+τHCCC(33)
867	-	-	τ HCCC(55)
859	844	843	γ OCNC (13)
827	827	-	γ OCOC (13)
802	816	-	δOCN(13)+δCCC(18)
766	749	750	δOCO(13)
693	694	-	υ CCC(16)+ δ OCO(35)
667	634		υ CCC(75)
630	607	635	υ OCN(10)
511	553	529	γ NCCC (12)+ γ OCNC(12)
457	457	-	υ CCN(11)
376	-	-	υ CCC(20)
260	-	-	υ CCC(10)
224	-	-	υ CCN(12)

υ–Stretching;δ–in-plane-bending;τ–torsion;γ–out-of-plane-bending

Fig.1 Molecular structure of cefadroxilalong with numbering of atoms

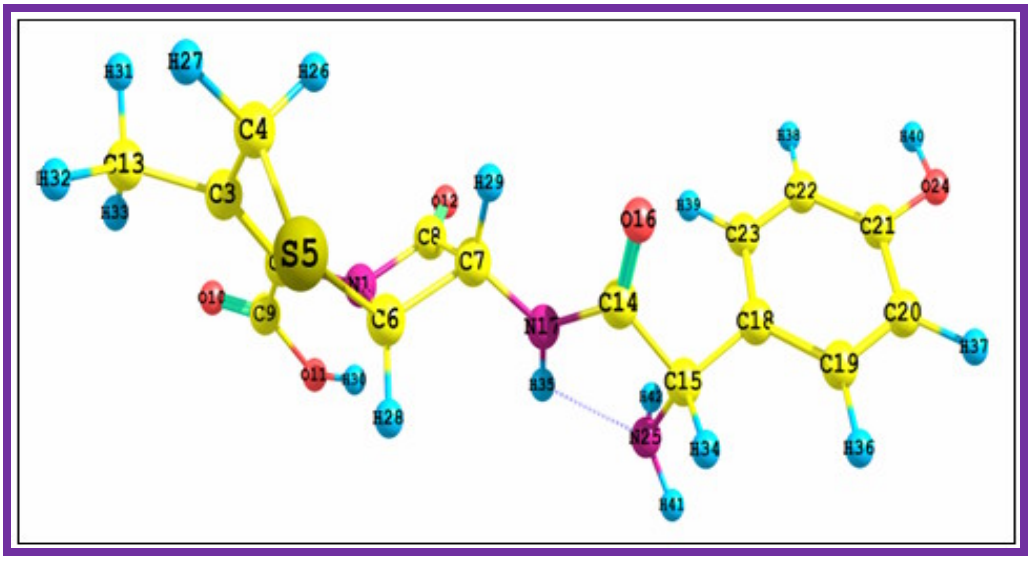

Fig.2 Molecular electrostatic potential of cefadroxil

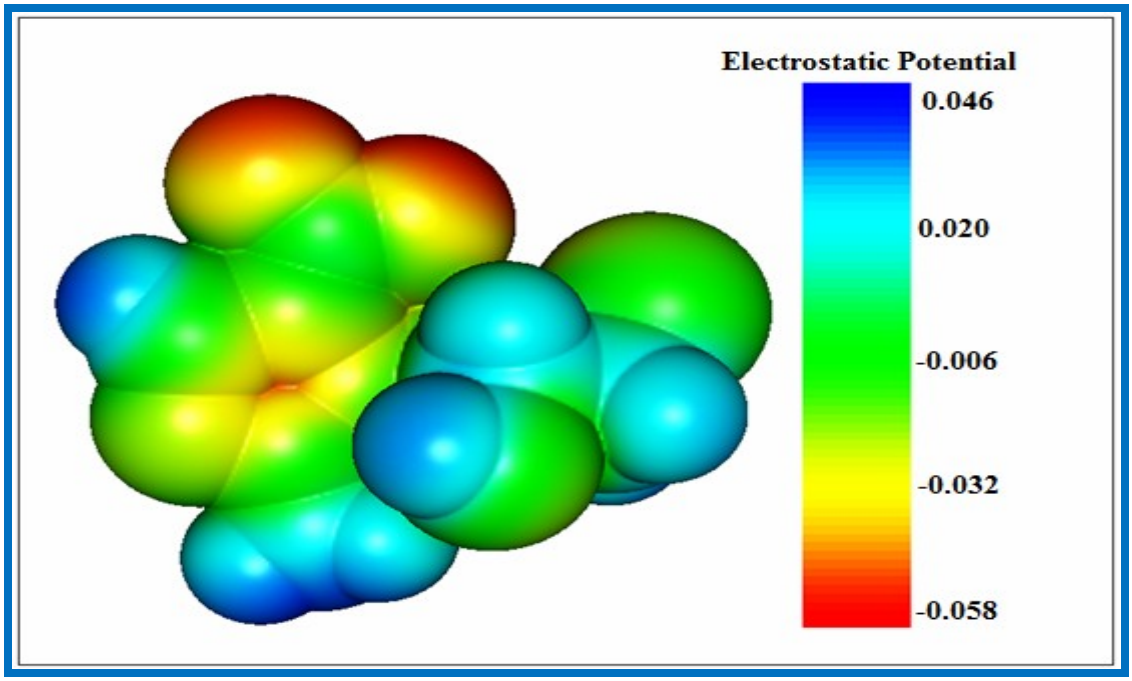

Fig.3 UV -Visible spectrum of CEfadroxil

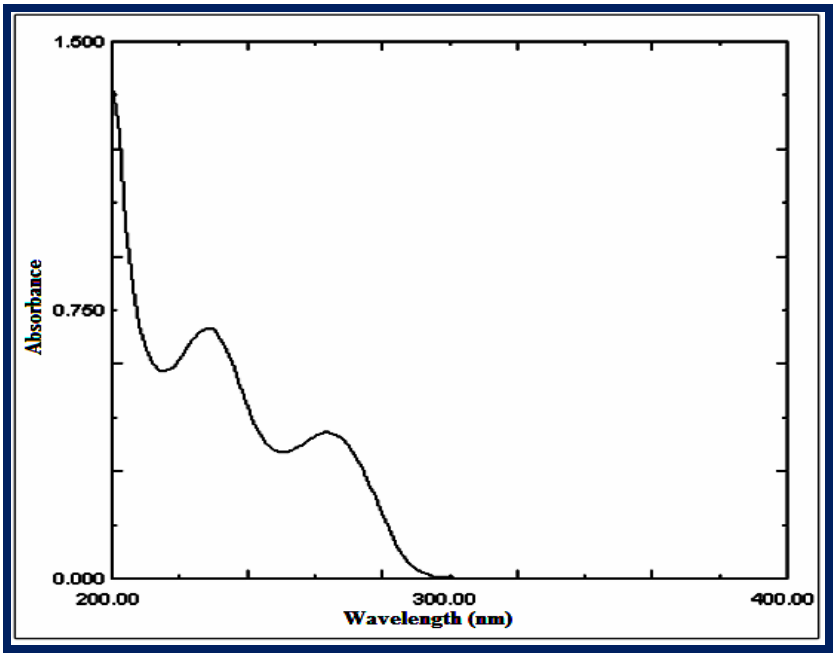

Fig.4 Natural population analysis chart of cefadroxil

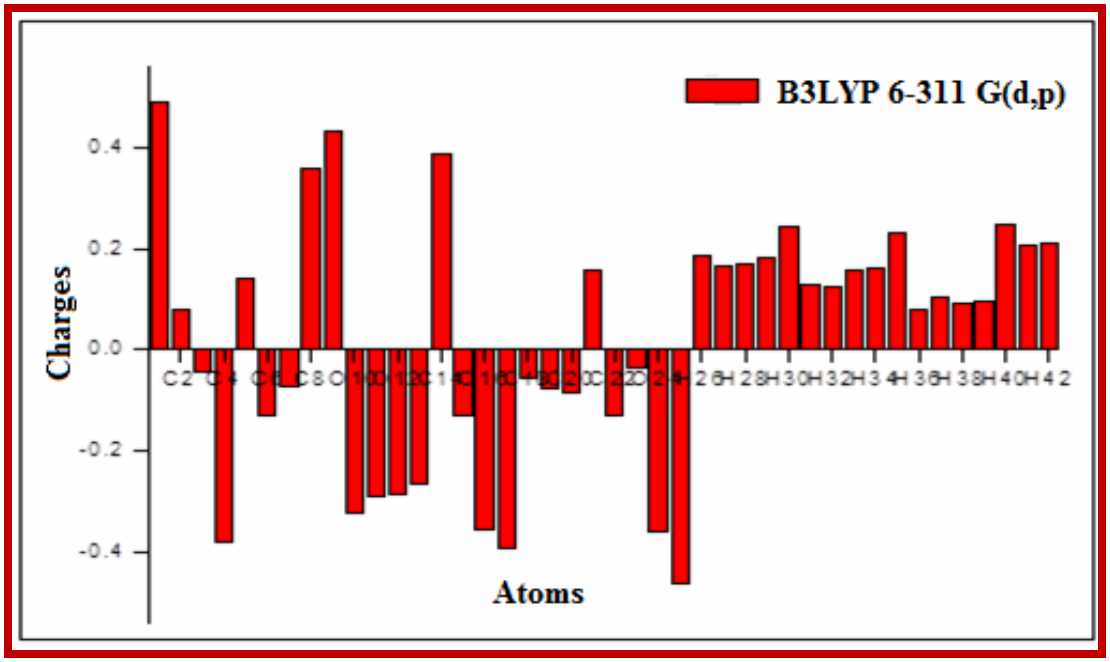

Fig.5 Correlation graph between thermodynamic parameters and temperature

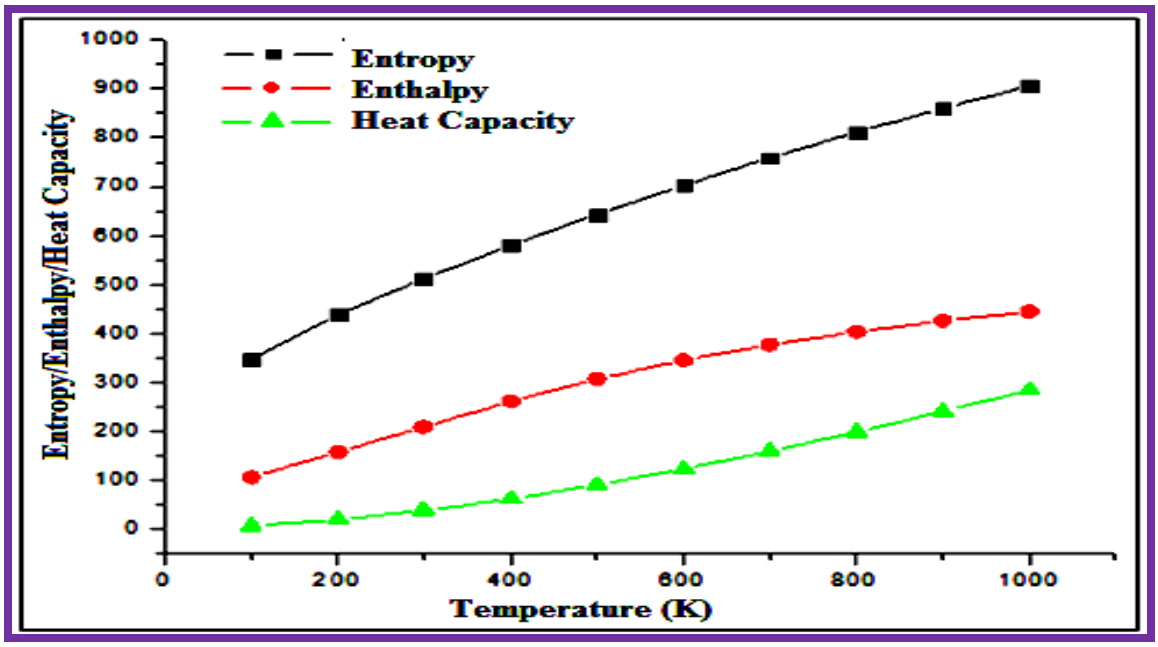

Fig.6 Frontier molecular orbital of cefadroxil

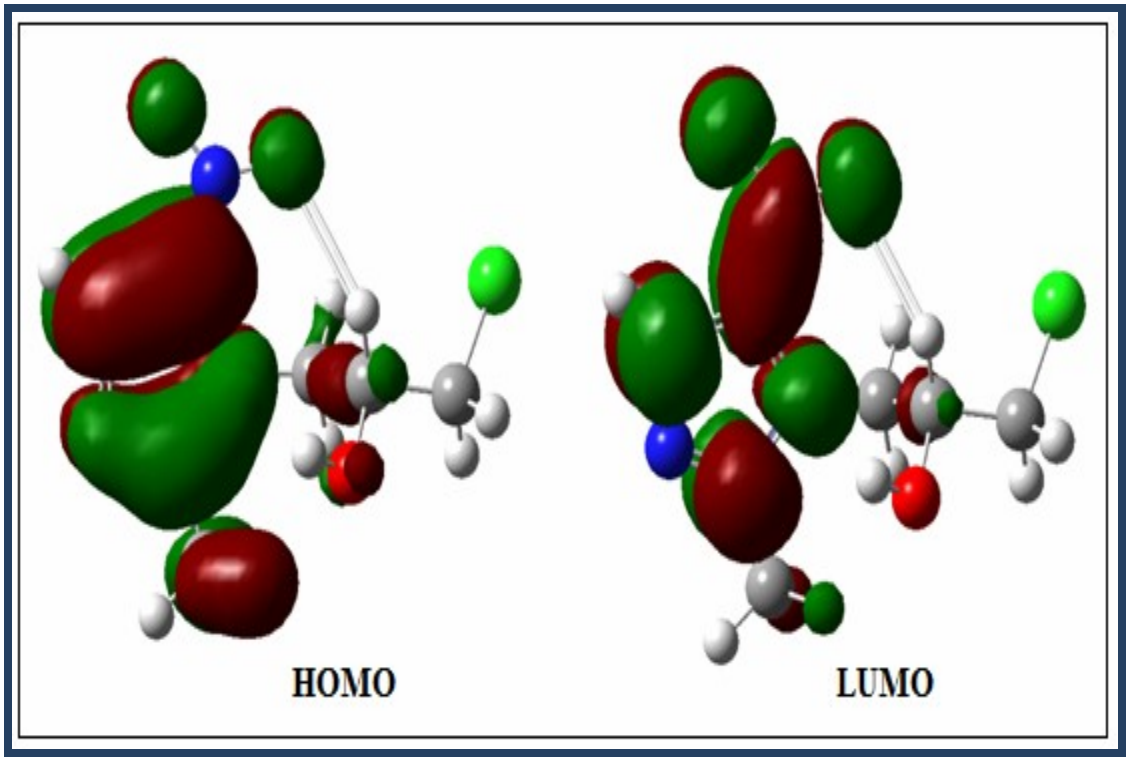

Fig.7 FT-Raman spectra of cefadroxil **Fig. 8** FT-IR spectra of cefadroxil

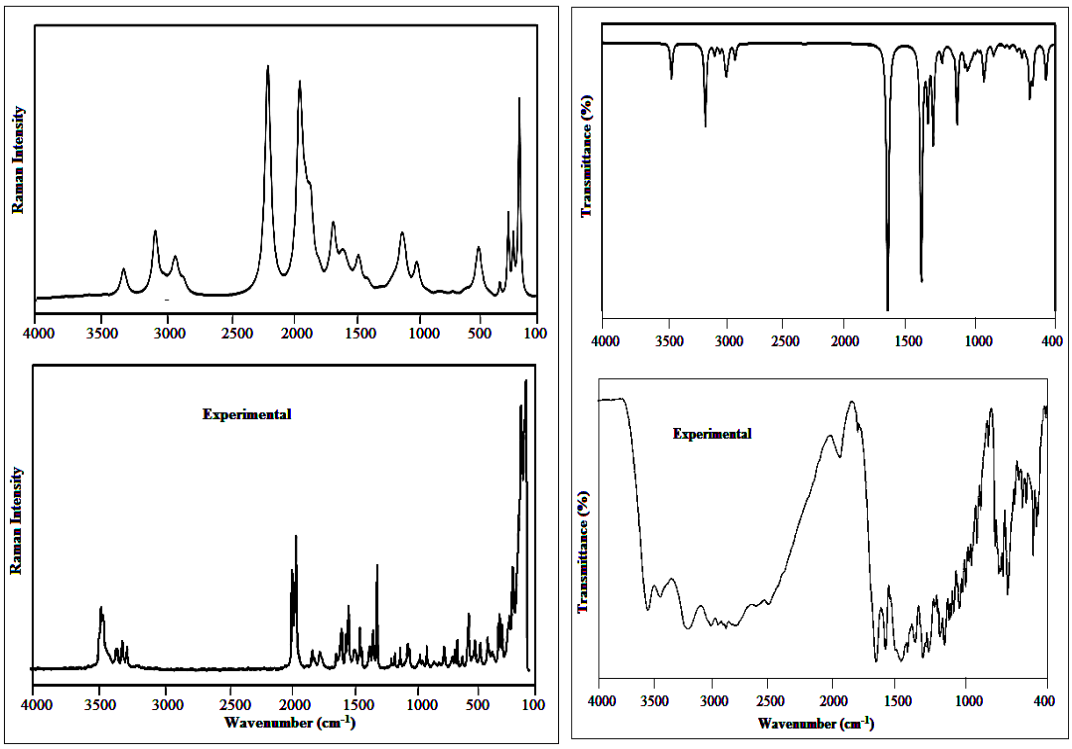

In conclusion, the vibrational FT-IR and FT-Raman spectra of cefadroxil were recorded and computed vibrational wavenumbers and their PED were calculated. The molecular structural parameters like bond length, bond angles, thermodynamic properties and vibrational frequencies of the fundamental modes of the optimized geometry have been determined from DFT calculations using B3LYP/6-311G (d,p) basis set. The electronic properties were also calculated and compared with the experimental UV–Vis spectrum. The calculated HOMO and LUMO energies were used to analyse the charge transfer within the molecule. The predicted MEP figure revealed the negative regions of the molecule, was subjected to the electrophilic attack of this compound.

References

Atalay, Y., Avil, D., Basaoglu, A. 2008. *Struct. Chem.*, 19: 239–243.

Auda, S.H., Mrestani, Y., Ahmed, A.M.S., Neubert, R.H.H. 2009. Characterization of the interaction of cefadroxil with different metal ions using capillary electrophoresis. *Electrophoresis*, 30: 1066–1070.

Becke, A.D. 1992. *J. Chem. Phys.*, 97: 9173–9177.

Becke, A.D. 1993. *J. Chem. Phys.*, 98: 5648–5652.

Erdogdu, Y., Unsalan, O., Amalanathan, M., Hubert Joe, I. 2010. *J. Mol. Struct.*, 980: 24–30.

Fliszar, S. 1983. Charge distributions and chemical effects. Springer, New York.

Frisch, A., Nielsen, A.B., Holder, A.J. 2003. Gauss view Users' Manual, Gaussian Inc.

Frisch, M.J., Trucks, G.W., Schlegel, H.B., Scuseria, *et al.* 2004. Gaussian 03W, Revision A02, Inc., Wallingford, CT.

Gece, G., Corros, 2008. *Science,* Pp. 502981–2992.

Gunasekaran, S., Ponnambalam, U., Muthu, S., Anand, G. 2004. *Indian J. Pure Appl. Physics*, 46: 162.

Hartstein, A.L., Patrick, K.E., Jones, S.R., Miller, M.J., Bryant, R.E. 1977. Comparison of pharmacological and antimicrobial properties of cefadroxil and cephalexin, *Antimicrob. Agents Chemother.,* 12: 93–97.

Irikura, K.K. 2002. THERMO.PERL Script, National Institute of Standards and Technology.

Jamroz, M.H. 2004. Vibrational Energy Distribution Analysis VEDA 4, Warsaw.

Jug. K., Maksic, Z.B. 1991. In: Maksic Z.B. (Ed.), Theoretical model of chemical bonding, Part – 3. Springer, Berlin. Pp. 233–238.

Krishnakumar, V., Sundarasan, N., Natarajan, A. 1994. *Asian J. Phy.*, PP. 3167.

Lee, C., Yang, W., Parr, R.G. 1988. *Phys. Rev. B.*, 37: 785–789.

Lewis, D.F.V., Ioannides, C., Parke, D.V. 1994. *Xenobiotica,* 24: 401–408.

Monasterios, Milagros Avendano, Mari'a Isabel Amaro, Wilson Ifante, Jamie Charris, 2006. *J. Mol. Struct.,* 798: 102–108.

Mrozek-Lyszczek, R. 2004. Thermal investigations of cefadroxil complexes with transition metals. Coupled TG-DSC and TG-FTIR techniques. *J. Thermal Anal. Calorim.*, 78: 473–486.

Padmaja, L., Ravikumar, C., Sajan, D., Joe, I.H., Jayakumar, V.S., Petti, G.R., Nelson, OF. 2009. *J. Raman Spectrosc.*, 40: 419–428.

Pfeffer, M., Jackson, A., Ximenes, J., Perche de Menezes, J. 1977. Comparative human oral clinical pharmacology of cefadroxil, cephalexin, and

cephradine. *Antimicrob. Agents Chemother.*, 11: 331–338.

Pihlaja, K., Kleinpeter, E. (Eds), 1994. Carbon-13 chemical shifts in structural and stereo chemical analysis, VCH Publishers, Deerfield Beach.

Rajesh, P., Gunasekaran, S., Seshadri, S., Gnanasambandan, T. 2014. *Spectrochimca Acta*, 132: 249–255.

Sagdinc, S., Pir, H. 2009. *Spectrochim. Acta A*, 73: 181–187.

Silverstein, R.M., Webster, F.X., Kiemle, D.J. 2009. Spectrometric identification. of organic compounds.

Snehalatha, M., Ravikumar, C., Joe, I.H., Jayakumar, V.S. 2009a. *J. Raman Spectrosc.*, 40: 1121–1126.

Snehalatha, M., Ravikumar, C., Joe, I.H., Sekar, N., Jayakumar, VS. 2009b *Spectrochim. Acta A*, 72: 654–662.

Sundaraganesan, N., Ilakiamani, S., Joshua, B.D. 2007. *Spectrochim. Acta A* 67: 287–297.

Uesugi, Y., Mizuno, M., Shimojima, A., Takahashi, H. 1997. *J. Phys. Chem.*, 101: 268–274.

Varsanyi, G. 1974. Assignments for vibrational spectra of seven hundred bezene derivatives, Vols.1-2, Adom Hilger.

Vijayakumar, T., Hubertjoe, I., Nair, C.P.R., Jaya Kumar, V.S. 2008. *Chem. Phys.* 343: 83–89.

Zayed, M.A., Abdallah, S.M. 2004. Synthesis, characterization and electronic spectra of cefadroxil complexes of d-block elements.Spectrochim. Acta Part A 60: 2215– 2224.